Probing Phase Coupling Between Two Spin-Torque Nano-Oscillators with an External Source

Yi Li,[1,*] Xavier de Milly,[1] Flavio Abreu Araujo,[2] Olivier Klein,[3] Vincent Cros,[2] Julie Grollier,[2] and Grégoire de Loubens[1,†]

[1]*Service de Physique de l'État Condensé, CEA, CNRS, Université Paris-Saclay, 91191 Gif-sur-Yvette, France*
[2]*Unité Mixte de Physique CNRS, Thales, Univ. Paris-Sud, Université Paris-Saclay, 91767 Palaiseau, France*
[3]*SPINTEC, Université Grenoble Alpes, CEA, CNRS, 38000 Grenoble, France*

Phase coupling between auto-oscillators is central for achieving coherent responses such as synchronization. Here we present an experimental approach to probe it in the case of two dipolarly coupled spin-torque vortex nano-oscillators using an external microwave field. By phase locking one oscillator to the external source, we observe frequency pulling on the second oscillator. From coupled phase equations we show analytically that this frequency pulling results from concerted actions of oscillator-oscillator and source-oscillator couplings. The analysis allows us to determine the strength and phase shift of coupling between two oscillators, yielding important information for the implementation of large interacting oscillator networks.

Self-sustained oscillators that are linked by phase coupling exhibit abundant collective dynamics [1] and describe diverse systems in nature [2–10]. In particular, they can synchronize, which is important in the fields of engineering, biology, and computing. Indeed, synchronized oscillators exhibit improved amplitudes and spectral purity of their outputs, and can be used to study and mimic neural networks [11,12]. Theoretical explorations of this phenomenon have been going on for decades, in particular within the framework of the Kuramoto model [13,14], where phase coupling is simplified as a sinusoidal function of phase difference,

$$\frac{d\varphi_i}{dt} = \omega_i + \sum_j \Omega_{ji} \sin(\varphi_j - \varphi_i + \beta_i), \quad (1)$$

where φ_i is the phase of the ith oscillator, ω_i is its free-running frequency, Ω_{ji} is the coupling strength between the jth and ith oscillators, and β_i is an intrinsic phase shift related to the nature of the coupling and to the nonlinearity of the oscillator [15]. In experiments, technological progress has allowed mutual synchronization in many systems compatible with lithographic fabrications, such as Josephson junctions [2], nanomechanical and optomechanical structures [3–5], and spin-torque nano-oscillators [6,7,16–19]. The strength of synchronization in all these systems is set by the coupling parameters in Eq. (1). However, the coupling strength Ω_{ji} and the intrinsic phase shift β_i are rarely quantified in experiments despite their importance for achieving large phase-locking ranges [20,21]. Being able to quantify these parameters is also crucial for synchronization-based information processing such as coupled-oscillator associative memories [22,23].

Among different oscillator systems, spin-torque nano-oscillators [24] serve as outstanding candidates for implementing coupled oscillator arrays, due to their submicron dimensions, nonlinear behaviors with large frequency tunability, simple signal extractions from magneto-resistance, and ease of being coupled and synchronized [6,7,16–19,25–30]. Of special engineering interests are spin-torque vortex oscillators [31,32], which allow operation without biasing field and different tuning properties [33–35] linked to the bistable orientation of the vortex core magnetization (polarity) [36]. The synchronization of two adjacent vortex oscillators through their dipolar field [37–39] has been demonstrated [18,40–42], as has the control of the phase-locking bandwidth by their relative vortex polarities [18,43]. Moreover, vortex oscillators are a model system for coupled oscillators in general, because their dynamics is well understood [44] and their phase coupling can be described by Kuramoto-like equations [18,45].

In this Letter we employ a third reference "oscillator," namely, an external microwave field with tunable frequency and power, as a dynamical probe to measure the dipolar coupling between two spin-torque vortex oscillators. When the microwave field phase locks one oscillator, an obvious frequency pulling is measured on the second oscillator. By including the coupling to external source in Eq. (1), we show analytically that this frequency pulling is due to in-phase actions of source-oscillator and interoscillator couplings within the phase-locking bandwidths, beyond which it disappears. The model is tested upon varying the source-oscillator coupling by changing the microwave power, and the interoscillator coupling by changing the vortex polarity states. It allows us to extract dipolar coupling strengths and phase shifts, with the former compatible with analytical calculations [43]. Our results provide a new way to directly reveal and characterize the mutual coupling between oscillators through their attraction to a third reference oscillator, which can be applied to various oscillator systems.

Our sample consists of two cylindrical spin-torque nano-oscillators with identical nominal diameters of $2R = 400$ nm and an edge-to-edge separation of $L = 200$ nm, as shown in
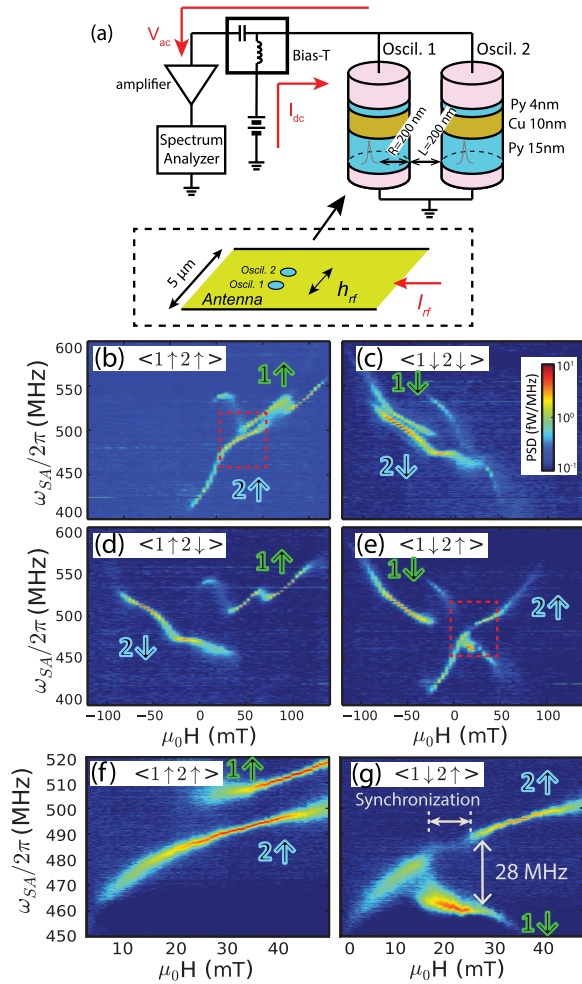
FIG. 1.   (a) Schematics of the sample and electrical circuit. (b)–(g) Power spectral density maps of auto-oscillation modes in log scale. Four different polarity states of the two thick Py vortex layers are shown: (b) $\langle 1\uparrow 2\uparrow\rangle$, (c) $\langle 1\downarrow 2\downarrow\rangle$, (d) $\langle 1\uparrow 2\downarrow\rangle$, and (e) $\langle 1\downarrow 2\uparrow\rangle$. (f),(g) Enlarged power spectral density data of $\langle 1\uparrow 2\uparrow\rangle$ and $\langle 1\downarrow 2\uparrow\rangle$ for the red box regions of (b) and (e), respectively. Mutual synchronization is observed between $\mu_0 H = 17.5$ and 26.0 mT in the $\langle 1\downarrow 2\uparrow\rangle$ state.

Fig. 1(a). Each oscillator has a spin-valve layer structure of Py(15 nm)|Cu(10 nm)|Py(4 nm) (Py = $Ni_{80}Fe_{20}$). During operation a strong dc current is injected through the two oscillators in parallel, which favors a vortex state in all Py layers [46]. It flows from Py(4 nm) to Py(15 nm), so that in each oscillator the spin-transfer torque destabilizes the mode dominated by the thick layer and overdamps the thin-layer dynamics [33,34,47]. The current is set to 95 mA, i.e., 1.5 times the critical current to drive the auto-oscillations of the thick Py layers. The dynamics excited in each oscillator corresponds to the rotation of the vortex core around its equilibrium position, the so-called gyrotropic mode [48]. Because of the small lateral separation, the two oscillators are dynamically coupled through their dipolar field [18,40]. We note that, owing to their much smaller volumes and limited dynamics, the contribution of the thin-layer vortices to the

oscillator-oscillator coupling is weak. Moreover, their vortex core polarity is not purposely controlled in this study. In the following, we will thus refer exclusively to the vortices in the thick Py layers of each oscillator, labeled 1 and 2. To provide an external rf field, an electrically isolated antenna is patterned on top of the sample [49], creating an in-plane $h_{\rm rf}$ linearly polarized along the direction made by the two oscillators [see Fig. 1(a)]. Furthermore, a biasing magnetic field is applied perpendicular to the sample plane in order to vary the gyrotropic frequencies [36,44].

First, we examine the microwave signals associated with auto-oscillations in each oscillator. Figures 1(b)–1(e) show the color maps of the power spectral density as a function of perpendicular field H. In each graph, two branches corresponding to the gyrotropic modes of the thick-layer vortex in each oscillator are observed. The four combined vortex polarity states for oscillators 1 and 2 can be obtained after applying well-chosen perpendicular switching fields [33]. The polarity state of oscillator i is defined as $\langle i\uparrow\rangle$ ($\langle i\downarrow\rangle$) for vortex core magnetization parallel (antiparallel) to the positive biasing field direction, which corresponds to a positive (negative) frequency-field slope [36,44].

Next we demonstrate the existence of dipolar coupling by the observation of mutual synchronization. Figures 1(f) and 1(g) compare the enlarged power spectra of the $\langle 1\uparrow 2\uparrow\rangle$ and $\langle 1\downarrow 2\uparrow\rangle$ states for $0 \leq \mu_0 H \leq 50$ mT, as labeled by the red boxes in Figs. 1(b) and 1(e), respectively. By switching the polarity of vortex oscillator 1, a clear gap of the auto-oscillation branch for oscillator 2 is found between $\mu_0 H = 17.5$ and 26 mT in the $\langle 1\downarrow 2\uparrow\rangle$ state, while for the $\langle 1\uparrow 2\uparrow\rangle$ state the branch is continuous. This gap, accompanied by a bright lower-frequency branch, is associated to the synchronization of the two oscillators. From the right edge of the synchronization bandwidth, we deduce that the maximal frequency mismatch for mutual synchronization is 28 MHz. The frequency mismatch corresponding to the unlocking of the two oscillators at the left edge is smaller. We attribute this to the fact that the amplitude and linewidth of oscillators can vary with the perpendicular field [34], which will change the effective dipolar coupling. The results above show that the dipolar interaction is strong enough to synchronize the two oscillators. Still, a quantitative evaluation of its strength Ω_{ji} and phase shift β_i is lacking at this point of the analysis.

In order to directly reveal and quantify the dipolar coupling, we fix both the biasing current and magnetic field and apply a weak microwave field, which couples to both oscillators. The two oscillators are set to an unsynchronized state at $\mu_0 H = 31.9$ mT, shown in Fig. 2(a). Figure 2(b) shows the evolution of auto-oscillation peaks of the two oscillators as a function of the external microwave field frequency ω_e. When ω_e crosses the peak of oscillator 1 around 460 MHz, the disappearance of the peak reflects the phase locking to the external rf source [25,26,29]. In addition, we also detect a significant frequency pulling on
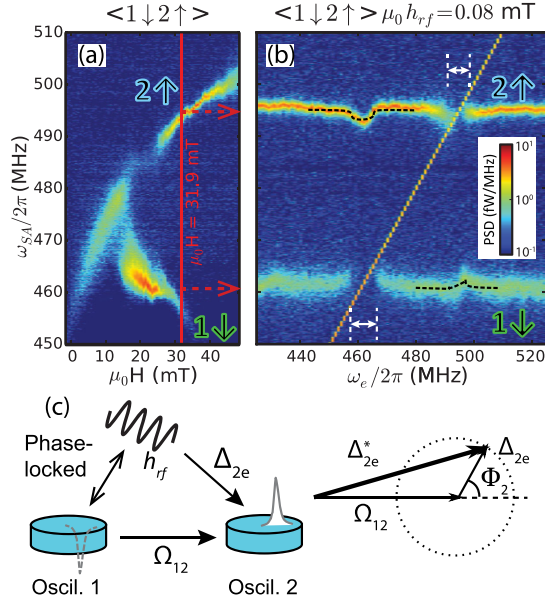
FIG. 2.   (a) Location of spectra at the $\langle 1{\downarrow}2{\uparrow}\rangle$ state for the microwave study. (b) Auto-oscillation spectra as a function of microwave field frequency for $\mu_0 H = 31.9$ mT, indicated in (a). Signal from the source appears as the oblique narrow line. The microwave power is -23 dBm, corresponding to $\mu_0 h_{\rm rf} = 0.08$ mT. White arrows show the phase-locking bandwidths. Black dashed curves are the fits to Eq. (4). (c) Vector diagram of Ω_{12} and Δ_{2e} when oscillator 1 is phase locked to the microwave field.

oscillator 2. This is a striking observation, because the frequency mismatch between oscillators, $(\omega_2 - \omega_1)/2\pi = 35$ MHz, is 5 times larger than the phase-locking bandwidths, around 7 MHz, of the two oscillators to the external source. The remote frequency pulling is a strong indication of coupling between the two oscillators as it is bound to the phase-locking bandwidth. It is important to note that no obvious frequency shift is observed when ω_e lies between the two auto-oscillation peaks. Reciprocally, a similar effect is also observed on oscillator 1 when oscillator 2 is phase locked to the microwave field around 495 MHz.

To understand these phenomena, we develop a simplified analytical formalism based on general oscillator equations [15]. For two dipolarly coupled vortex oscillators experiencing a linearly polarized microwave field, the phase equations can be formulated [46] from the Thiele equation which describes the vortex core dynamics in a magnetic dot [50–52], as

$$-\frac{d\theta_i}{dt} + \omega_e - \omega_{ig} + \Omega_{ji} \cos(\theta_i + \gamma_i^{\rm nl} - \theta_j)$$
$$- \Delta_{ie} \sin(\theta_i + \gamma_i^{\rm nl} + \gamma_i^{\rm rf}) = 0, \qquad (2)$$

where $\theta_i = \omega_e t - p_i \varphi_i$ is the phase difference between the microwave field and the position of the vortex core, $p_i = \pm 1$ is the vortex polarity, ω_{ig} is the free-running frequency of oscillator i, $\Omega_{ji} = \Omega(X_j/X_i)$ is the dipolar coupling strength

Ω normalized by the ratio of vortex gyration amplitudes X_j/X_i, and Δ_{ie} is the coupling strength to the external microwave source. The index is defined as $(i, j) = (1, 2)$ or $(2, 1)$. In Eq. (2) two additional phases are present: $\gamma_i^{\rm nl}$ is the intrinsic phase shift introduced by the nonlinearity of the oscillators [15,20] and $\gamma_i^{\rm rf}$ is the microwave coupling phase, which is determined by the geometric alignment of the microwave field to each oscillator [see Fig. 1(a)]. We highlight that Eq. (2) describes the general behaviors of self-sustained oscillators: for $\Delta_{ie} = 0$, it is reduced to Kuramoto equations Eq. (1) with $\beta_i = \pi/2 - \gamma_i^{\rm nl}$, where the $\pi/2$ phase originates from the conservative nature of dipolar coupling [15]; for $\Omega = 0$, it is reduced to the Adler equation responsible for one oscillator phase locking to an external source [53].

In the general case, the phase dynamics of oscillator 2 evolves in a complex way due to the uncorrelated forces exerted by the microwave field and oscillator 1. However, when oscillator 1 phase locks to the microwave field, the situation simplifies: its relative phase with respect to the microwave field, θ_1, becomes a constant. In that case, we can rewrite the phase dynamics of oscillator 2 in Eq. (2) as driven solely by the action of the microwave field, but with a modified effective coupling strength Δ_{2e}^* that takes into account both the microwave coupling and the dipolar attraction to oscillator 1,

$$\Delta_{2e}^* = \sqrt{\Delta_{2e}^2 + \Omega_{12}^2 - 2\Delta_{2e}\Omega_{12} \cos \Phi_2}. \qquad (3)$$

From Eq. (3), we find Δ_{2e}^* is the vector sum of the effective dipolar coupling strength Ω_{12} and the microwave coupling strength Δ_{2e} with a phase difference $\Phi_2 = \theta_1 + \gamma_2^{\rm rf} + \pi/2$ [Fig. 2(c)]. The frequency of oscillator 2 is then determined by the frequency of the microwave field and the strength of this new effective coupling Δ_{2e} through

$$\omega_2 = \omega_e \pm \sqrt{(\omega_e - \omega_{2g})^2 - (\Delta_{2e}^*)^2}, \qquad (4)$$

where $\pm$ depends on the sign of $\omega_e - \omega_{2g}$. Equation (4) indicates that when oscillator 1 is phase locked to the microwave field, it can help pull the frequency of oscillator 2 towards the frequency of the source, as observed in Fig. 2(b).

Full analytical solutions to our model can be obtained in the limit of weak microwave coupling [46]. In Fig. 3 we use them to extract the coupling parameters under different conditions. First, the microwave power is varied, which sets the phase-locking bandwidths and associated remote frequency pullings. Second, both antiparallel (AP) [Figs. 3(a) and 3(b)] and parallel (P) [Figs. 3(c) and 3(d)] vortex polarity alignments are examined, for which the strength of dipolar coupling is expected to change by a factor close to 3 [18,43]. The data are fitted to Eq. (4) with Ω and $\gamma_i^{\rm nl}$ as the fit parameters. Positive and negative signs of Ω are expected for parallel and antiparallel polarity alignments, respectively
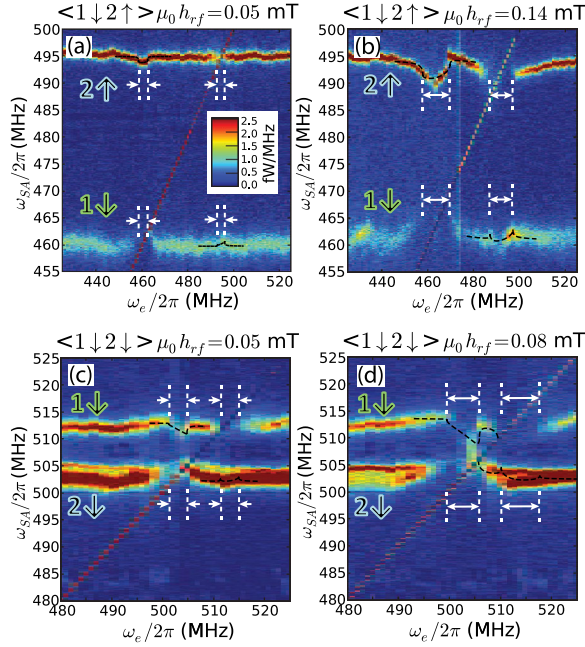
FIG. 3.   Probing dipolar coupling in various conditions. (a),(b) The $\langle 1\downarrow 2\uparrow \rangle$ state for $\mu_0 H = 31.9$ mT, with microwave powers of (a) -28 dBm and (b) -18 dBm. (c),(d) The $\langle 1\downarrow 2\downarrow \rangle$ state for $\mu_0 H = -61.6$ mT with microwave power of (c) -28 dBm and (d) -23 dBm. White arrows show the phase-locking bandwidths. Black dashed curves are the fits to Eq. (4). The fit parameters are listed in Table I.

[43], which is taken into account. Details about the fitting procedure can be found in the Supplemental Material [46]. The fitting curves are shown in Fig. 3 and Fig. 2(b).

Table I lists the fitting results along with the microwave field amplitude $h_{\rm rf}$. As expected, the mean of phase-locking strengths $(\Delta_{1e} + \Delta_{2e})/2$ is proportional to the microwave field. For the antiparallel polarity alignment, the extracted dipolar coupling Ω slightly increases with $h_{\rm rf}$. One reason is that the vortex gyration amplitude X_i might be increased as oscillator i is phase-locked to the microwave field, resulting in an enhancement of Ω_{ij} on oscillator j. Another possibility is the incomplete phase locking at small $h_{\rm rf}$ [observed in Fig. 3(a) for oscillator 2] due to thermal fluctuations, which are likely to reduce the effective coupling [26,29]. Owing to

TABLE I.   Fit parameters of Figs. 2(b) and 3. The values of $h_{\rm rf}$ are calculated from the antenna geometry. The signs of Ω are fixed to the predictions in Ref. [43].

	Antiparallel			Parallel	
$\mu_0 h_{\rm rf}$ (mT)	0.05	0.08	0.14	0.05	0.08
$\frac{\Delta_{1e}+\Delta_{2e}}{4\pi}$ (MHz)	1.8	3.2	5.5	1.8	3.5
$\Omega/2\pi$ (MHz)	-6.7	-7.9	-9.3	3.6	4.2
$\gamma_1^{\rm nl}$ (rad)	-2.7	-2.8	-2.0	2.6	2.1
$\gamma_2^{\rm nl}$ (rad)	1.1	1.1	0.7	-2.1	-1.4

these two counteracting effects, we take the average of the three experiments, $\Omega_{\rm AP}/2\pi = -8.0$ MHz, as the extracted value of Ω. For the parallel polarity state, we take the value extracted from Fig. 3(c), $\Omega_{\rm P}/2\pi = 3.6$ MHz, as the strength of the dipolar coupling. In fact, the limit of weak microwave coupling does not hold in Fig. 3(d) because of the large microwave power in comparison to the small frequency mismatch between oscillators; this results in a more complex dynamics. It is interesting to note that the two values compare favorably with the ones obtained from the macrodipole approximation taking into account solely the thick Py layers [40,43]. In that case, $\Omega_{\rm AP(P)}/2\pi = -3(+1) \times \xi^2 \gamma \mu_0 M_s R^2 h/32\pi d^3 = -6.9(2.3)$ MHz, where $\xi = 2/3$ from the two-vortex ansatz [48], $\gamma/2\pi = 29.7$ GHz/T is the gyromagnetic ratio, $\mu_0 M_s = 0.96$ T is the saturation magnetization of the Py vortex layers [49], h is their thickness, and $d = 2R + L$ is the center-to-center distance between oscillators. We also point out that the ratio $\Omega_{\rm AP}/\Omega_{\rm P}$ in our experiment agrees with the ratio of critical frequency mismatch in our prior work, $\Delta f_{\rm AP}/\Delta f_{\rm P} = 2.4$ [18], and depends on the exact geometry of the oscillator pair [43].

The phase shift $\gamma_i^{\rm nl}$ is linked to the position of the largest remote frequency pulling in Fig. 3. In the antiparallel polarity alignment, the values of $\gamma_i^{\rm nl}$ are reproducible at various microwave fields but differ from those in the parallel alignment, indicating large variations of parameters in magnetic dynamics upon polarity change. From the model, $\tan \gamma_i^{\rm nl}$ is the reduced nonlinear coefficient ν_i of oscillator i [15]. However, we note that the fitting results with negative values of $\gamma_i^{\rm nl}$ point towards either an additional extrinsic phase due to, e.g., parasitic rf couplings between the antenna and sample circuits, or more complex dynamics than assumed in the simple analytical model.

One interesting finding is that the extracted Ω in the antiparallel polarity alignment is much smaller than the phase-locking frequency mismatch of 28 MHz found in Fig. 1(g). In our experiments the amplitude ratio X_2/X_1 is close to 1 [46]. In the phase-locking solution derived by Slavin and Tiberkevich [54], the maximal frequency mismatch for mutual synchronization is then $\Omega(\nu_1 + \nu_2)$. Thus we confirm the role of nonlinearities, with $\nu_1 + \nu_2$ around 3.5, in the large phase-locking frequency mismatch. The fact that the synchronized mode is closer to the peak branch of oscillator 1 likely indicates that ν_2 is greater than ν_1, making it easier for oscillator 2 to adapt its frequency to oscillator 1.

Our results show that two dipolarly coupled spin-torque vortex oscillators follow ideal oscillator systems described by Eq. (2), a preassumption for studies based on the Kuramoto model [45]. We confirm that the dipolar coupling strength can be tuned by a factor greater than 2 with bistable polarity states [18,43], providing a unique freedom to manipulate the collective dynamics. For instance, a new propagating wave mode has been predicted in oscillator arrays with both attracting and repulsive interactions [55],

which can be realized with the two different polarity alignments. In addition, we learn about the nonlinearities in spin-torque nano-oscillators. Finite phase shifts γ_i^{nl} are measured, as predicted in theory [15,56] and as identified in similar systems [19,30]. This indicates that practical oscillator networks fall into the Sakaguchi-Kuramoto regime [Eq. (1) with nonzero β_i)] in which synchronization can be destroyed by the phase detunings at medium Ω [21].

In summary, we have developed a novel approach to study coupled oscillators with an external ac drive. By controlling the relative phases between the ac source and one phase-locked oscillator, we acquire not only the strength but also the phase information of the interoscillator coupling. This probing technique is not restricted to spin-torque oscillators and microwave field, but is applicable to all coupled oscillator systems and ac drives. By extending our understanding of them, this technique is also useful for further manipulation and investigation of collective dynamics in large arrays of auto-oscillators.

---

[*] yi.li@cea.fr
[†] gregoire.deloubens@cea.fr

[1] A. Pikovsky, M. Rosenblum, and J. Kurths, *Synchronization: A Universal Concept in Nonlinear Sciences* (Cambridge University Press, Cambridge, England, 2001).
[2] K. Wiesenfeld, P. Colet, and S. H. Strogatz, Phys. Rev. Lett. **76**, 404 (1996).
[3] S.-B. Shim, M. Imboden, and P. Mohanty, Science **316**, 95 (2007).
[4] G. Heinrich, M. Ludwig, J. Qian, B. Kubala, and F. Marquardt, Phys. Rev. Lett. **107**, 043603 (2011).
[5] M. Zhang, G. S. Wiederhecker, S. Manipatruni, A. Barnard, P. McEuen, and M. Lipson, Phys. Rev. Lett. **109**, 233906 (2012).
[6] S. Kaka, M. R. Pufall, W. H. Rippard, T. J. Silva, S. E. Russek, and J. A. Katine, Nature (London) **437**, 389 (2005).
[7] F. B. Mancoff, N. D. Rizzo, B. N. Engel, and S. Tehrani, Nature (London) **437**, 393 (2005).
[8] I. Z. Kiss, Y. Zhai, and J. L. Hudson, Science **296**, 1676 (2002).
[9] M. R. Tinsley, S. Nkomo, and K. Showalter, Nat. Phys. **8**, 662 (2012).
[10] L. H. Hartwell, J. J. Hopfield, S. Leibler, and A. W. Murray, Nature (London) **402**, C47 (1999).
[11] N. Locatelli, V. Cros, and J. Grollier, Nat. Mater. **13**, 11 (2013).
[12] J. Grollier, D. Querlioz, and M. D. Stiles, Proc. IEEE **104**, 2024 (2016).
[13] Y. Kuramoto, *Chemical Oscillations, Waves, and Turbulence* (Springer, Berlin, 1984).
[14] J. A. Acebrón, L. L. Bonilla, C. J. Pérez-Vicente, F. Ritort, and R. Spigler, Rev. Mod. Phys. **77**, 137 (2005).
[15] A. Slavin and V. Tiberkevich, IEEE Trans. Magn. **45**, 1875 (2009).
[16] A. Ruotolo, V. Cros, B. Georges, A. Dussaux, J. Grollier, C. Deranlot, R. Guillemet, K. Bouzehouane, S. Fusil, and A. Fert, Nat. Nanotechnol. **4**, 528 (2009).
[17] S. Sani, J. Persson, S. M. Mohseni, Y. Pogoryelov, P. K. Muduli, A. Eklund, G. Malm, M. Käll, A. Dmitriev, and J. Åkerman, Nat. Commun. **4**, 2731 (2013).
[18] N. Locatelli, A. Hamadeh, F. A. Araujo, A. D. Belanovsky, P. N. Skirdkov, R. Lebrun, V. V. Naletov, K. A. Zvezdin, M. Muñoz, J. Grollier, O. Klein, V. Cros, and G. de Loubens, Sci. Rep. **5**, 17039 (2015).
[19] R. Lebrun, S. Tsunegi, P. Bortolotti, H. Kubota, A. S. Jenkins, M. Romera, K. Yakushiji, A. Fukushima, J. Grollier, S. Yuasa, and V. Cros, arXiv:1601.01247.
[20] V. Tiberkevich, A. Slavin, E. Bankowski, and G. Gerhart, Appl. Phys. Lett. **95**, 262505 (2009).
[21] O. E. Omel'chenko and M. Wolfrum, Phys. Rev. Lett. **109**, 164101 (2012).
[22] G. Csaba, M. Pufall, D. Nikonov, G. Bourianoff, A. Horvath, T. Roska, and W. Porod, in 2012 13th International Workshop on Cellular Nanoscale Networks and Their Applications (CNNA) (IEEE, Turin, Italy, 2012), pp. 1–2.
[23] D. E. Nikonov, G. Csaba, W. Porod, T. Shibata, D. Voils, D. Hammerstrom, I. A. Young, and G. I. Bourianoff, IEEE J. Explor. Solid-State Comput. Devices Circuits **1**, 85 (2015).
[24] S. I. Kiselev, J. C. Sankey, I. N. Krivorotov, N. C. Emley, R. J. Schoelkopf, R. A. Buhrman, and D. C. Ralph, Nature (London) **425**, 380 (2003).
[25] W. H. Rippard, M. R. Pufall, S. Kaka, T. J. Silva, S. E. Russek, and J. A. Katine, Phys. Rev. Lett. **95**, 067203 (2005).
[26] B. Georges, J. Grollier, M. Darques, V. Cros, C. Deranlot, B. Marcilhac, G. Faini, and A. Fert, Phys. Rev. Lett. **101**, 017201 (2008).
[27] S. Urazhdin, P. Tabor, V. Tiberkevich, and A. Slavin, Phys. Rev. Lett. **105**, 104101 (2010).
[28] M. Quinsat, J. F. Sierra, I. Firastrau, V. Tiberkevich, A. Slavin, D. Gusakova, L. D. Buda-Prejbeanu, M. Zarudniev, J.-P. Michel, U. Ebels, B. Dieny, M.-C. Cyrille, J. A. Katine, D. Mauri, and A. Zeltser, Appl. Phys. Lett. **98**, 182503 (2011).
[29] A. Hamadeh, N. Locatelli, V. V. Naletov, R. Lebrun, G. de Loubens, J. Grollier, O. Klein, and V. Cros, Appl. Phys. Lett. **104**, 022408 (2014).
[30] R. Lebrun, A. Jenkins, A. Dussaux, N. Locatelli, S. Tsunegi, E. Grimaldi, H. Kubota, P. Bortolotti, K. Yakushiji, J. Grollier, A. Fukushima, S. Yuasa, and V. Cros, Phys. Rev. Lett. **115**, 017201 (2015).
[31] V. S. Pribiag, I. N. Krivorotov, G. D. Fuchs, P. M. Braganca, O. Ozatay, J. C. Sankey, D. C. Ralph, and R. A. Buhrman, Nat. Phys. **3**, 498 (2007).
[32] A. Dussaux, B. Georges, J. Grollier, V. Cros, A. V. Khvalkovskiy, A. Fukushima, M. Konoto, H. Kubota, K. Yakushiji, S. Yuasa, K. A. Zvezdin, K. Ando, and A. Fert, Nat. Commun. **1**, 8 (2010).
[33] N. Locatelli, V. V. Naletov, J. Grollier, G. de Loubens, V. Cros, C. Deranlot, C. Ulysse, G. Faini, O. Klein, and A. Fert, Appl. Phys. Lett. **98**, 062501 (2011).

[34] A. Hamadeh, N. Locatelli, V. V. Naletov, R. Lebrun, G. de Loubens, J. Grollier, O. Klein, and V. Cros, Phys. Rev. Lett. **112,** 257201 (2014).

[35] V. Sluka, A. Kákay, A. M. Deac, D. E. Bürgler, C. M. Schneider, and R. Hertel, Nat. Commun. **6,** 6409 (2015).

[36] G. de Loubens, A. Riegler, B. Pigeau, F. Lochner, F. Boust, K. Y. Guslienko, H. Hurdequint, L. W. Molenkamp, G. Schmidt, A. N. Slavin, V. S. Tiberkevich, N. Vukadinovic, and O. Klein, Phys. Rev. Lett. **102,** 177602 (2009).

[37] J. Shibata, K. Shigeto, and Y. Otani, Phys. Rev. B **67,** 224404 (2003).

[38] S. Sugimoto, Y. Fukuma, S. Kasai, T. Kimura, A. Barman, and Y. C. Otani, Phys. Rev. Lett. **106,** 197203 (2011).

[39] D.-S. Han, A. Vogel, H. Jung, K.-S. Lee, M. Weigand, H. Stoll, G. Schütz, P. Fischer, G. Meier, and S.-K. Kim, Sci. Rep. **3,** 2262 (2013).

[40] A. D. Belanovsky, N. Locatelli, P. N. Skirdkov, F. A. Araujo, J. Grollier, K. A. Zvezdin, V. Cros, and A. K. Zvezdin, Phys. Rev. B **85,** 100409(R) (2012).

[41] A. D. Belanovsky, N. Locatelli, P. N. Skirdkov, F. A. Araujo, K. A. Zvezdin, J. Grollier, V. Cros, and A. K. Zvezdin, Appl. Phys. Lett. **103,** 122405 (2013).

[42] F. A. Araujo and J. Grollier, J. Appl. Phys. **120,** 103903 (2016).

[43] F. A. Araujo, A. D. Belanovsky, P. N. Skirdkov, K. A. Zvezdin, A. K. Zvezdin, N. Locatelli, R. Lebrun, J. Grollier, V. Cros, G. de Loubens, and O. Klein, Phys. Rev. B **92,** 045419 (2015).

[44] A. Dussaux, A. V. Khvalkovskiy, P. Bortolotti, J. Grollier, V. Cros, and A. Fert, Phys. Rev. B **86,** 014402 (2012).

[45] V. Flovik, F. Macià, and E. Wahlström, Sci. Rep. **6,** 32528 (2016).

[46] See Supplemental Material at http://link.aps.org/supplemental/10.1103/PhysRevLett.118.247202 for details, which presents additional experimental data, analytical derivations and data fitting procedure.

[47] A. V. Khvalkovskiy, J. Grollier, N. Locatelli, Y. V. Gorbunov, K. A. Zvezdin, and V. Cros, Appl. Phys. Lett. **96,** 212507 (2010).

[48] K. Y. Guslienko, B. A. Ivanov, V. Novosad, Y. Otani, H. Shima, and K. Fukamichi, J. Appl. Phys. **91,** 8037 (2002).

[49] V. V. Naletov, G. de Loubens, G. Albuquerque, S. Borlenghi, V. Cros, G. Faini, J. Grollier, H. Hurdequint, N. Locatelli, B. Pigeau, A. N. Slavin, V. S. Tiberkevich, C. Ulysse, T. Valet, and O. Klein, Phys. Rev. B **84,** 224423 (2011).

[50] K. Y. Guslienko, Appl. Phys. Lett. **89,** 022510 (2006).

[51] B. A. Ivanov and C. E. Zaspel, Phys. Rev. Lett. **99,** 247208 (2007).

[52] A. V. Khvalkovskiy, J. Grollier, A. Dussaux, K. A. Zvezdin, and V. Cros, Phys. Rev. B **80,** 140401(R) (2009).

[53] R. Adler, Proc. IRE **34,** 351 (1973).

[54] A. N. Slavin and V. S. Tiberkevich, Phys. Rev. B **74,** 104401 (2006).

[55] H. Hong and S. H. Strogatz, Phys. Rev. Lett. **106,** 054102 (2011).

[56] Y. Zhou, J. Persson, and J. Åkerman, J. Appl. Phys. **101,** 09A510 (2007).